Acta Cryst A
FOUNDATIONS
ADVANCES

ISSN 2053-2733

Isogonal non-crystallographic periodic graphs based on knotted sodalite cages

Olaf Delgado-Friedrichs,[a] Michael O'Keeffe[b] and Michael M. J. Treacy[c]*

[a]Department of Applied Mathematics, Australian National University, Canberra, ACT 2601, Australia, [b]School of Molecular Sciences, Arizona State University, Tempe, Arizona 85287, USA, and [c]Department of Physics, Arizona State University, Tempe, Arizona 85287, USA. *Correspondence e-mail: treacy@asu.edu

Received 6 August 2020
Accepted 21 September 2020

Edited by J.-G. Eon, Universidade Federal do Rio de Janeiro, Brazil

Keywords: knotted zeolite frameworks; linked zeolite frameworks; non-crystallographic symmetry; *Systre*.

Supporting information: this article has supporting information at journals.iucr.org/a

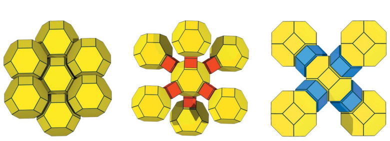

This work considers non-crystallographic periodic nets obtained from multiple identical copies of an underlying crystallographic net by adding or flipping edges so that the result is connected. Such a structure is called a 'ladder' net here because the 1-periodic net shaped like an ordinary (infinite) ladder is a particularly simple example. It is shown how ladder nets with no added edges between layers can be generated from tangled polyhedra. These are simply related to the zeolite nets **SOD**, **LTA** and **FAU**. They are analyzed using new extensions of algorithms in the program *Systre* that allow unambiguous identification of locally stable ladder nets.

1. Introduction

We describe a series of knotted spatial graphs (embeddings of abstract graphs) based on linkages of truncated octahedra ('sodalite cages'). They were inspired by the observation that replacing the six-membered rings (6-rings) in the net of faujasite by knotted 12-rings (trefoil knots) produced the remarkable 'knotted faujasite' framework, **qlg**, shown in Fig. 1.

Embedded graphs are generally assigned RCSR (Reticular Chemistry Structure Resource) symbols (O'Keeffe *et al.*, 2008), which are three letters in lower-case bold (for example, the truncated octahedron symbol is **toc**). Graphs that correspond to the nets of zeolite frameworks also have the IUPAC symbol which is three-letter upper-case bold – for example the net of the zeolite faujasite is the zeolite framework-type code **FAU** (Baerlocher *et al.*, 2007).

The standard approach to the characterization of periodic graphs is that of the program *Systre* (Delgado-Friedrichs, 2005; Delgado-Friedrichs & O'Keeffe, 2003; Delgado-Friedrichs *et al.*, 2017). In this approach, vertices of a periodic graph are given barycentric (center-of-mass) coordinates. It is easy to show (Delgado-Friedrichs, 2005) that if coordinates, say (0, 0, 0), are assigned to one vertex in a periodic net relative to unit-cell axes, the rest are unique. It can be shown also (Delgado-Friedrichs, 2005) that barycentric coordinates are the same as the equilibrium configuration that would result at fixed volume if vertices were linked by equal harmonic springs, so such a configuration is called an 'equilibrium placement'. It may happen that in such a placement two or more vertices have the same barycentric coordinates (a 'collision'). The structure is then considered 'unstable'. If distinct neighbors of the same vertex in the structure always have distinct barycentric coordinates, it is 'locally stable'; in particular, all stable structures are also locally stable. The simplest kind of local instability occurs when two vertices have the same neighbors and, accordingly, identical barycentric coordinates.

Table 1
Data for the embedded graphs.

Under ‘vertices’ and ‘edges’ are the transitivity of the embedding with transitivity of the underlying graph in parentheses.

Symbol	Parent	Symmetry	Linkage	Vertices	Edges	Symbol
qlp	**toc**	432	NL	2 (1)	3 (2)	$4.10_8.10_8$
qlz	**toc**	432	LL	2 (1)	4 (2)	$4.10_8.10_8$
toc-c	**toc**	432	LN	2 (1)	3 (2)	4.6.6
qle	**SOD**	*I*432	NL	1 (1)	1 (1)	$4.4.10_{16}.10_{16}.10_{16}.10_{16}$
qlh	**SOD**	*I*432	LL	1 (1)	2 (1)	$4.4.10_{16}.10_{16}.10_{16}.10_{16}$
qlf	**LTA**	*P*432	NL	2 (1)	4 (3)	$4.8.4.10_8.4.10_8$
lta-c	**LTA**	*P*432	NN	2 (1)	5 (3)	4.6.4.6.4.8
qlg	**FAU**	$F4_132$	NL	4 (1)	9 (4)	$4.4.4.10_8.10_8.12$
qlk	**FAU**	$F4_132$	LN	4 (1)	9 (4)	$4.6.6.6.6_2.8_2$
qlj	**FAU**	$Fd\bar{3}$	NL	4 (1)	8 (4)	$4.6.6.8_2.6.8_2$
fau-c	**FAU**	$Fd\bar{3}$	LN	4 (1)	8 (4)	4.4.4.6.6.12

The automorphisms of the graph then include interchange of the two vertices – an operation variously described as a ‘local symmetry’, ‘non-rigid-body symmetry’ or ‘non-crystallographic symmetry’. The last term arises because the automorphism group of the graph is not isomorphic with a crystallographic symmetry group. *Systre* also produces a unique ‘*Systre* key’, which allows unambiguous determination of whether two crystallographic nets are the same or are different graphs (Delgado-Friedrichs *et al.*, 2017).

In this work we are concerned with structures in which no non-crystallographic symmetries associated with local instabilities as above occur, but for which, in barycentric coordinates, each vertex collides with at least one other that is symmetry-equivalent to it. Such structures, which are also necessarily non-crystallographic, are called ‘ladders’ and are not treated by the current version of *Systre*. However, recent extensions (to be published) of the *Systre* algorithms allow generation of *Systre* keys for locally stable ladder nets provided that collisions only occur in pairs. These developments were applied to the nets reported herein. Non-crystallographic periodic nets (those that have an automorphism group that is not isomorphic to a space group) are always unstable (Moreira de Oliveira & Eon, 2011, 2013, 2014). The converse is not necessarily true: crystallographic nets may be unstable (Eon, 2011; Delgado-Friedrichs *et al.*, 2013). In the terminology used by Eon *et al.* what we call a ladder here could be described as a periodic graph in which the group of ‘bounded’ automorphisms (*i.e.* those for which the distance between a vertex and its image is bounded) acts freely (without fixed points) on the vertices and has non-trivial elements of finite order (Eon, 2011; Moreira de Oliveira & Eon, 2011, 2013, 2014).

A useful intrinsic property of graphs, such as those of zeolite nets, is the vertex symbol (O’Keeffe & Hyde, 1997) which gives the size and number of the shortest ring at each vertex.

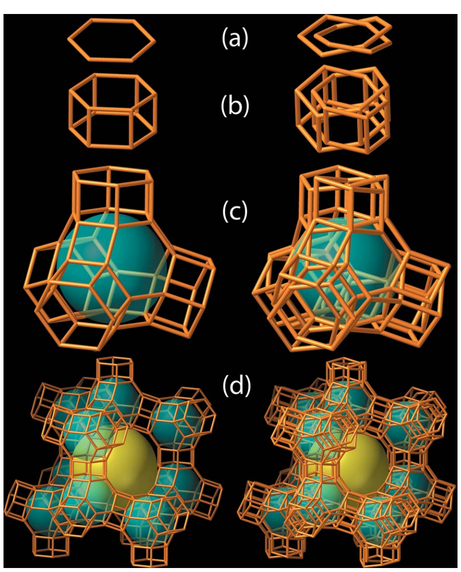

Figure 1
Left column. The **FAU** framework type can be constructed by assembling (*a*) 6-rings into (*b*) 6-ring prisms. (*c*) Prisms cross-connect to enclose truncated octahedra (**toc**, sodalite cages) in the interior space, and (*d*) these cross-connect, by sharing prisms, to form the **FAU** framework. Right column. The knotted-**FAU** framework (**qlg**) can be constructed by assembling (*a*) 12-ring trefoils into (*b*) knotted double-6-ring prisms. (*c*) These cross-link, as for **FAU**, to form (*d*) the knotted **FAU** framework, **qlg**.

2. Generation and description of ladder nets

We start with a pair of concentric truncated octahedra (*i.e.* sodalite cages, symmetry 432) and link them together as shown in Fig. 2. As may be seen in the figure, pairs of 4-rings can be linked in a 4-crossing Solomon link. Likewise, pairs of 6-rings can be connected to form a torus-knotted 12-ring (actually the 6-crossing trefoil knot). The possibilities (N = not linked, L = linked) are NN = two separate polyhedra, LN = two catenated polyhedra **toc-c**, NL and LL, and in both latter cases the ‘polyhedra’ with vertex symbol $4.10_8.10_8$ are assigned RCSR symbols **qlp** and **qlz**, respectively. These last three have embeddings (shown) with symmetry 432 (*O*). It should be apparent that, as abstract graphs, **qlp** and **qlz** are isogonal (vertex-transitive) and indeed have the same vertex symbol (Table 1) and are the same graph in two topologically distinct embeddings (not ‘ambient isotopic’). This is because, although in the 432 embedding there are two vertices, from the point of view of an abstract graph there is an automorphism, interchanging the inner and outer sets of vertices. This vertex-

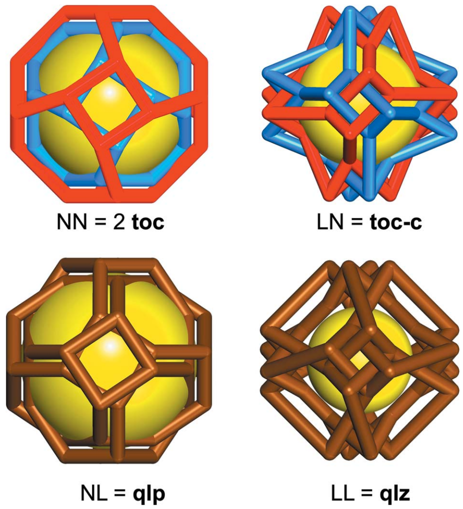

Figure 2
Modes of linkage for nestled pairs of sodalite cages.

transitivity, of course, does not correspond to a rigid-body symmetry.

Turning now to 3-periodic structures, we note that packing truncated octahedra into a simple tiling produces the sodalite framework **SOD** as shown in Fig. 3. Linking truncated octahedra and cubes produces the zeolite framework **LTA** and linking truncated octahedra with hexagonal prisms produces the faujasite framework **FAU**, as also shown in the figure. Note that we restrict ourselves to the simplest possibility of one type of large cage in each structure.

Structures derived from **SOD** (Fig. 4) are **qle** (NL) and **qlh** (LL). **qle**, like **SOD**, is a vertex- and edge-transitive graph (transitivity 1 1). **qle** and **qlh** both have the same vertex symbol (Table 1) and the updated *Systre* program confirms that these indeed have the same graph.

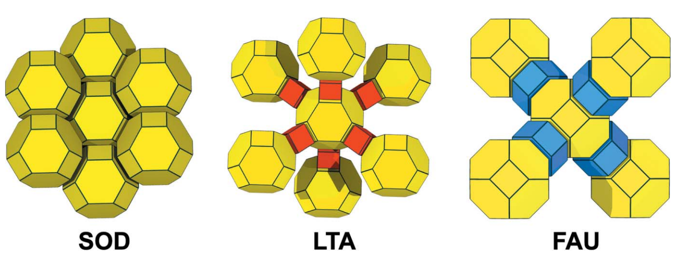

Figure 3
Zeolite frameworks with truncated octahedra (**toc**, sodalite cages).

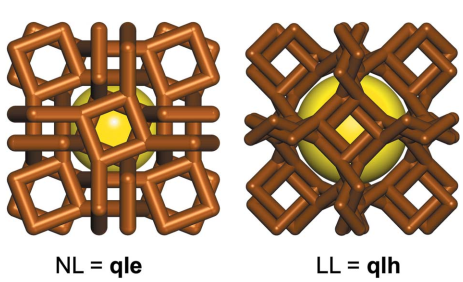

Figure 4
Structures based on the **SOD** framework.

We also find two structures based on the **lta** pattern with the maximum possible symmetry $P432$ (Fig. 5). The first (NN) is two distinct interwoven **LTA** nets (RCSR symbol for the embedding **lta-c**). The second (NL) **qlf** has transitivity 2 5 in the embedding shown; however, the *Systre* analysis shows that the graph transitivity is actually 1 3 and, further, that the symmetry is a double extension of $Pm\overline{3}m$ (*i.e.* an order-2 non-crystallographic supergroup of $Pm\overline{3}m$). However (as also shown in the figure), an embedding in $Pm\overline{3}m$ results in intersecting edges in pairs of 6-rings, and therefore is unfeasible with rigid sticks.

In the **FAU** net (symmetry $Fd\overline{3}m$) there are two sodalite cages in the primitive cell. For a structure with chiral double cages the maximum symmetry is 23 and the possible symmetries of the periodic structures are $F4_132$ (all cages of the same hand) and $Fd\overline{3}$ (cages of opposite hand). We find four possibilities shown in Fig. 6. One is a pair of interwoven **FAU** nets (**fau-c**). The other three have distinct graphs, as can be seen from the vertex symbols in Table 1 (in each case, for a given embedding, all vertices have the same vertex symbol). *Systre* analysis shows that all these structures have symmetries (not necessarily the same) that are double extensions of $Fd\overline{3}m$, and that all graphs with embeddings in the higher crystallographic symmetry ($Fd\overline{3}m$) require merging of pairs of vertices into one, reducing the vertex transitivity from 4 to 2, and again resulting inevitably in intersecting edges.

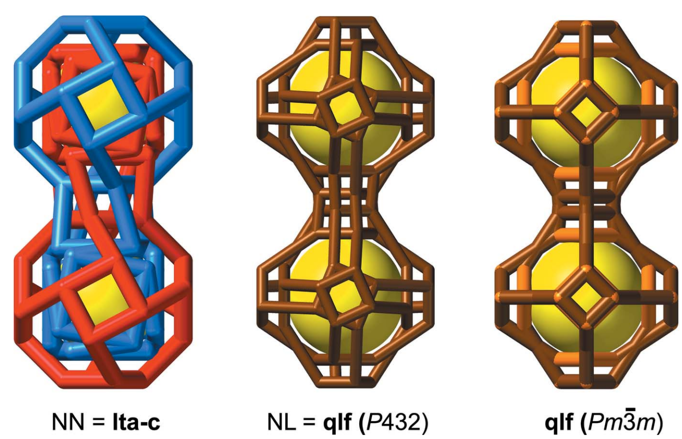

Figure 5
Structures based on the **LTA** framework. The higher-symmetry version of **qlf** on the right has intersecting straight edges of the 6-rings.

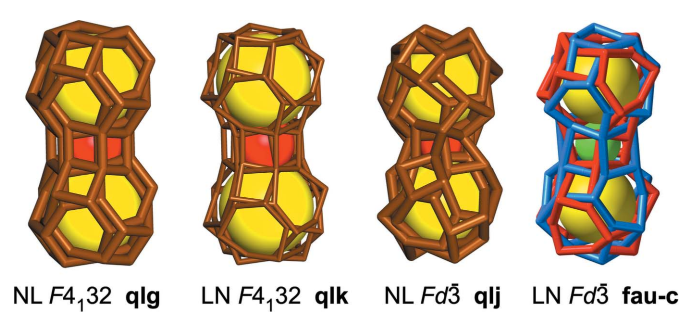

Figure 6
Structures based on the **FAU** framework.

Other patterns of entanglement may exist at lower symmetry, but are unlikely to be vertex-transitive, and we have not explored those possibilities.

3. Summary and conclusions

We have generated a number of isogonal non-crystallographic nets based on linked, tangled, truncated octahedra. The most symmetrical crystallographic embeddings that avoid intersecting edges are chiral, but they have achiral crystallographic embeddings with intersecting edges. We note that these knotted and linked nets are related to those of zeolites of first importance in materials chemistry. Although they cannot be plausibly synthesized as silicates, they do present a challenging, but feasible, problem for synthesis by reticular chemistry methods.

A beta version of *Systre* that includes treatment of ladder nets is available at https://github.com/odf/gavrog/releases/tag/Systre-20.8.0.

References

Baerlocher, C., McCusker, L. B. & Olson, D. H. (2007). *Atlas of Zeolite Framework Types*, 6th ed. Amsterdam: Elsevier Science.

Delgado-Friedrichs, O. (2005). *Discrete Comput. Geom.* **33**, 67–81.

Delgado-Friedrichs, O., Hyde, S. T., Mun, S.-W., O'Keeffe, M. & Proserpio, D. M. (2013). *Acta Cryst.* A**69**, 535–542.

Delgado-Friedrichs, O., Hyde, S. T., O'Keeffe, M. & Yaghi, O. M. (2017). *Struct. Chem.* **28**, 39–44.

Delgado-Friedrichs, O. & O'Keeffe, M. (2003). *Acta Cryst.* A**59**, 351–360.

Eon, J.-G. (2011). *Acta Cryst.* A**67**, 68–86.

Moreira de Oliveira, M. & Eon, J.-G. (2011). *Acta Cryst.* A**67**, 240–251.

Moreira de Oliveira, M. & Eon, J.-G. (2013). *Acta Cryst.* A**69**, 276–288.

Moreira de Oliveira, M. & Eon, J.-G. (2014). *Acta Cryst.* A**70**, 217–228.

O'Keeffe, M. & Hyde, S. T. (1997). *Zeolites*, **19**, 370–374.

O'Keeffe, M., Peskov, M. A., Ramsden, S. J. & Yaghi, O. M. (2008). *Acc. Chem. Res.* **41**, 1782–1789.